

Generating sensor signals in isotropic noise fields

Emanuël A. P. Habets^{a)}

School of Engineering, Bar-Ilan University, Ramat-Gan, Israel, and Department of Electrical Engineering, Technion—Israel Institute of Technology, Haifa, Israel

Sharon Gannot

School of Engineering, Bar-Ilan University, Ramat-Gan, Israel

(Received 14 June 2007; revised 27 September 2007; accepted 27 September 2007)

Researchers in the signal processing community often require sensor signals that result from a spherically or cylindrically isotropic noise field for simulation purposes. Although it has been shown that these signals can be generated using a number of uncorrelated noise sources that are uniformly spaced on a sphere or cylinder, this method is seldom used in practice. In this paper algorithms that generate sensor signals of an arbitrary one- and three-dimensional array that result from a spherically or cylindrically isotropic noise field are developed. Furthermore, the influence of the number of noise sources on the accuracy of the generated sensor signals is investigated. © 2007 Acoustical Society of America. [DOI: 10.1121/1.2799929]

PACS number(s): 43.50.Ed, 43.60.Fg [EJS]

Pages: 3464–3470

I. INTRODUCTION

A spherically isotropic noise field has been shown to be a reasonable model for a number of practical noise fields that can be found in, for example, an office or car. Cylindrically isotropic noise fields are especially useful when, for example, the ceiling and floor in an enclosure are covered with a highly absorbing material.¹ Spherical and cylindrical noise fields are also known as three-dimensional (3D) and two-dimensional (2D) diffuse noise fields, respectively. Researchers in the signal processing community often require sensor signals that result from these noise fields for simulation purposes, e.g., for (superdirective) beamforming,^{2,3} adaptive noise cancellation,^{4,5} and source localization. From a physical point of view the noise signals can be generated using a number of uncorrelated noise sources that are uniformly spaced on a sphere^{4,6} or cylinder. This method is, however, seldom used in practice. Some researchers, for example, convolve two uncorrelated noise signals with a room impulse response (without direct path) to generate the sensor signals that result from a spherically isotropic noise field. However, using this method the spherical noise field is not accurately simulated.

In this paper we develop algorithms that generate sensor signals of an arbitrary one-dimensional (1D) and 3D array that result from a spherical or cylindrical noise field. Furthermore, the influence of the number of noise sources on the accuracy of the generated sensor signals is investigated.

In Sec. II we show that an isotropic noise field can be generated using equally spaced noise sources on a sphere and cylinder to generate 3D and 2D diffuse noise fields, respectively. The algorithms that can be used to efficiently generate the sensor signals are developed in Sec. III. In Sec. IV we compare the spatial coherence that results from the generated sensor signals with the theoretical spatial coherence. In Sec.

V we demonstrate the use of the generated sensor signals by analyzing the directivity index of a filter and sum beamformer. Conclusions are presented in Sec. VI.

II. BACKGROUND THEORY

The noise fields of interest in this paper are composed of a superposition of uncorrelated plane waves arriving at omnidirectional sensors from various directions. The spatial coherence can be calculated by integrating the effect of a single plane wave. Therefore, we begin by considering the effect of a single plane wave. The sensor signals that result from a plane wave arriving from angle ϕ (see Fig. 1) are related by

$$x_2(t) = x_1\left(t - \frac{\Delta}{c}\right), \quad (1)$$

where c denotes the sound velocity in ms^{-1} and $\Delta = d \cos(\phi)$ the path difference of the plane wave, where d denotes the distance between the sensors. The isotropic assumption implies that the power spectrum densities of the signals are independent of the location, i.e.,

$$S_{x_1}(\omega) = S_{x_2}(\omega). \quad (2)$$

Hence, the cross-power spectrum density is given by

$$S_{x_1x_2}(\omega) = S_{x_1}(\omega)e^{-j\omega/cd \cos(\phi)}. \quad (3)$$

The spatial coherence can now be calculated by taking the integral over all plane waves that originate from a surface area A , i.e.,

$$\gamma_{x_1x_2}(\omega) = \frac{\oint_A S_{x_1x_2}(\omega) dA}{\oint_A \sqrt{S_{x_1}(\omega)S_{x_2}(\omega)} dA}, \quad (4)$$

^{a)}Author to whom correspondence should be addressed. Electronic mail: e.habets@ieee.org

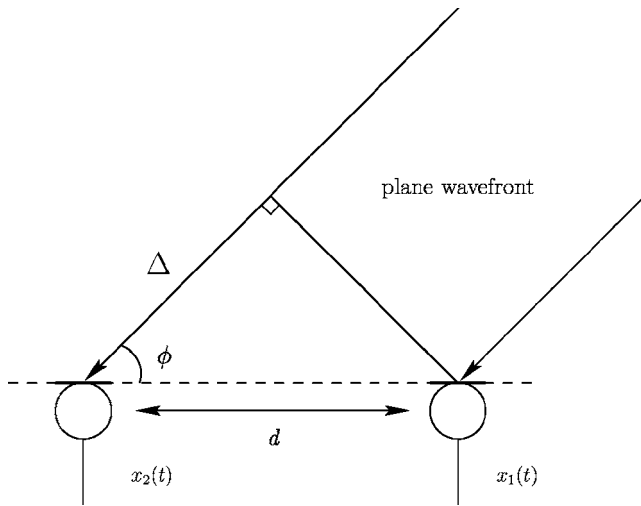


FIG. 1. Plane wave front impinging on an array of two sensors with an angle ϕ .

where dA denotes an infinitesimal area on a surface. Using Eqs. (2) and (3) we obtain

$$\gamma_{x_1 x_2}(\omega) = \frac{1}{A} \oint_A e^{-j\omega/cd \cos \phi} dA, \quad (5)$$

where A denotes the total surface area.

A. Spherically isotropic noise field

In case the sources are uniformly distributed on the surface of the sphere the integral in Eq. (5) can be evaluated over the surface area A of the sphere. Note that the plane wave assumption holds if the radius of the sphere r is much larger than the sensor distance d . Without loss of generality it is assumed that the sensors are positioned on the x axis. The infinitesimal area on the sphere $dA = r^2 \sin(\phi) d\phi d\theta$, and the surface of the sphere $A = 4\pi r^2$. In terms of the spherical coordinates $\phi \in [0, \pi]$ and $\theta \in [0, 2\pi)$ (see Fig. 2) we then obtain

$$\begin{aligned} \gamma_{x_1 x_2}(\omega) &= \frac{1}{4\pi r^2} \int_0^{2\pi} \int_0^\pi e^{-j\omega/cd \cos \phi} r^2 \sin(\phi) d\phi d\theta \\ &= \frac{1}{4\pi} \int_0^{2\pi} \int_0^\pi e^{-j\omega/cd \cos \phi} \sin(\phi) d\phi d\theta. \end{aligned} \quad (6)$$

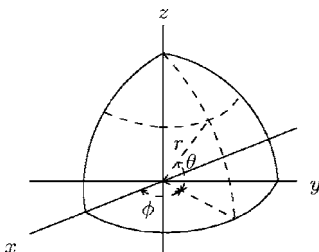


FIG. 2. Part of a sphere with radius r , azimuth ϕ , and elevation θ .

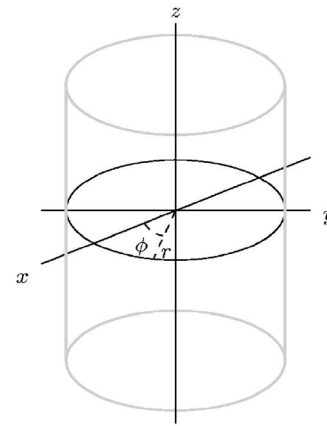


FIG. 3. Cylinder with radius r and cylindrical angle ϕ .

Now, using the substitution $g = \omega/cd \cos(\phi)$, we have

$$\gamma_{x_1 x_2}(\omega) = \frac{1}{2\omega d/c} \int_{-\omega d/c}^{\omega d/c} e^{-jg} dg = \frac{\sin(\omega d/c)}{\omega d/c}, \quad (7)$$

which is the well-known theoretical spatial coherence function for spherically isotropic noise and omni-directional sensors.⁷

B. Cylindrically isotropic noise field

In a cylindrically isotropic noise field the sources are uniformly distributed on the surface of a cylinder. It should be noted that all rings along the z axis of the cylinder have an equal contribution to the generated sensor signals. To derive the spatial coherence function in a cylindrical noise field the integral in Eq. (5) can be evaluated by integrating in one dimension, the cylindrical angle $\phi \in [0, 2\pi)$ (see Fig. 3). Note that $dA = rd\phi$ and $A = 2\pi r$. We then obtain⁸

$$\gamma_{x_1 x_2}(\omega) = \frac{1}{2\pi} \int_0^{2\pi} e^{-j\omega/cd \cos \phi} d\phi = J_0(\omega d/c), \quad (8)$$

where $J_0(\cdot)$ is the zero-order Bessel function of the first kind.

III. IMPLEMENTATION

In this section efficient algorithms are developed to generate the sensor signals of an arbitrary 3D and 1D array that result from a spherically and cylindrically isotropic noise field.

In the implementation we approximate the integral in Eq. (5) by a summation, i.e.,

$$\hat{\gamma}_{x_1 x_2}(\omega) = \frac{1}{N} \sum_{n=0}^{N-1} e^{-j\omega/cd \cos \phi_n}. \quad (9)$$

Note that the number of uncorrelated noise sources N should be sufficiently large to obtain a good approximation of the integral. We elaborate on the number of noise sources in Sec. IV.

The time delay (Δ/c) between the sensor signals depends on the location of the noise source. To efficiently implement this (fractional) delay the signals are generated in the Fourier domain. In this domain the delay can be modeled using a simple phase shift.

In the sequel it is assumed that the radius of the sphere or cylinder is much larger than the span of the sensor array such that all waves can be assumed to be plane waves.

A. Spherically isotropic noise field

The basic requirement is that the noise sources are uniformly distributed on the surface of the sphere, i.e., the probability that a noise source exists in each infinitesimal area should be equal. In that sense it should be understood that a uniform distribution of the noise sources with the spherical coordinates $\phi \in [0, \pi]$ and $\theta \in [0, 2\pi)$ does not result in the desired uniform distribution on the surface of the sphere. The probability that a noise source exists in each infinitesimal area on the sphere with spherical coordinates (ϕ, θ) is given by

$$P_r(\phi \leq \tilde{\phi} \leq \phi + d\phi, \theta \leq \tilde{\theta} \leq \theta + d\theta) = \frac{dA}{A} = \frac{1}{4\pi} \sin(\phi) d\phi d\theta. \quad (10)$$

The probability density function (pdf) of the surface area A can thus be expressed in terms of ϕ and θ as

$$p_A(\theta, \phi) = \frac{1}{4\pi} \sin(\phi). \quad (11)$$

This pdf can be factorized into two independent densities for ϕ and θ , such that

$$p_\phi(\phi) = \frac{1}{2} \sin(\phi) \text{ and } p_\theta(\theta) = \frac{1}{2\pi}. \quad (12)$$

Using the *inverse transform sampling method*⁹ we can generate ϕ and θ with the desired distributions using their cumulative densities, which are given by

$$P_\phi(\phi) = \frac{1}{2}(1 - \cos(\phi)) \text{ and } P_\theta(\theta) = \frac{\theta}{2\pi}, \quad (13)$$

respectively. Let $v_1 = P_\phi(\phi)$ and $v_2 = P_\theta(\theta)$ be independent uniform random variables on $[0, 1]$ and $[0, 1)$. Then, if we solve ϕ and θ we obtain

$$\phi = \arccos(1 - 2v_1) \quad (14)$$

and

$$\theta = 2\pi v_2, \quad (15)$$

which will have the desired pdfs given in Eq. (12).

1. 3D array

The M sensor positions, relative to the first sensor position, are stacked into a matrix \mathbf{P} such that

$$\mathbf{P} = \begin{bmatrix} 0 & x_2 & \dots & x_M \\ 0 & y_2 & \dots & y_M \\ 0 & z_2 & \dots & z_M \end{bmatrix}. \quad (16)$$

Each contributing noise signal is generated directly in the frequency domain. The path difference $\Delta(m, \phi, \theta)$ denotes the difference between the path lengths from the incident plane wave with direction (ϕ, θ) to the m th sensor and the first sensor. Its value is calculated by projecting the position vector of the m th sensor $\mathbf{P}(:, m)$ on the normal \mathbf{v} of the plane wave, i.e., $\Delta(m, \phi, \theta) = \mathbf{v}^T \mathbf{P}(:, m) / \|\mathbf{v}\|^2$. Since $\|\mathbf{v}\|^2 = 1$ we have

$$\Delta(m, \phi, \theta) = \mathbf{v}^T \mathbf{P}(:, m). \quad (17)$$

The M sensor signals of length L , denoted by \mathbf{Z} , that result from $N = N_\phi N_\theta$ uniformly distributed noise sources can be efficiently generated using Algorithm 1.

2. 1D array

For an arbitrary 1D array, i.e., with equally or non-equally spaced sensors, the algorithm can be simplified by exploiting the symmetry of the array. Without loss of generality it is assumed that the sensors of the array are positioned on the x axis. The sensor positions on the x axis relative to the first sensor are

$$\mathbf{p}_x = [0 \ x_2 \ \dots \ x_M]. \quad (18)$$

Since the sensors are located on the x axis the path difference Δ only depends on the azimuth $\tilde{\phi}$, i.e., all noise sources that lie on a ring with spherical coordinates $\phi = \tilde{\phi}$ and $\theta \in [0, 2\pi)$ result in the same path difference Δ . The path difference Δ is given by $d \cos(\phi)$, where d is the distance of the sensor with respect to the origin. For the m th sensor d is equal to $\mathbf{p}_x(m)$.

The M sensor signals of length L that result from N uniformly distributed noise sources can be generated using Algorithm 2.

B. Cylindrically isotropic noise field

In the previous section we dealt with spherically isotropic noise fields. However, it has been proposed that some room acoustic fields may be more closely modeled as a cylindrically isotropic noise field. Therefore, we develop an algorithm to generate the sensor signals that result from a cylindrical noise field.

Note that in this section the variable ϕ denotes the cylindrical angle $\phi \in [0, 2\pi)$.

Algorithm 1: Creating sensor signals for an arbitrary 3D array that result from a spherical noise field.

Data: \mathbf{P} , M , L , N_ϕ , N_θ , f_s

Result: \mathbf{Z}

$$L' = 2^{\lceil \log_2(L) \rceil};$$

$$\omega = \pi f_s \left[0 : \frac{1}{L'} : 1 \right];$$

$$\theta = 2\pi \left[0 : \frac{1}{N_\theta} : \frac{N_\theta - 1}{N_\theta} \right];$$

$$\phi = \arccos \left(1 - 2 \left[0 : \frac{1}{N_\phi - 1} : 1 \right] \right);$$

for $k=1: N_\phi$ **do**

for $l=1: N_\theta$ **do**

$$\mathbf{X}' = \text{randn}(1, L' + 1) + i \text{randn}(1, L' + 1);$$

$$\mathbf{X}(1, :) = \mathbf{X}(1, :) + \mathbf{X}';$$

$$\mathbf{v} = \begin{bmatrix} \cos(\theta(l)) \sin(\phi(k)) \\ \sin(\theta(l)) \sin(\phi(k)) \\ \cos(\phi(k)) \end{bmatrix};$$

for $m=2: M$ **do**

$$\Delta = \mathbf{v}^T \mathbf{P}(:, m);$$

$$\mathbf{X}(m, :) = \mathbf{X}(m, :) + \mathbf{X}' \exp(-j\Delta\omega/c);$$

end

end

end

$$\mathbf{X} = [\mathbf{X}(:, 1:L' + 1), \text{conj}(\mathbf{X}(:, L' : -1:2))];$$

$$\mathbf{Z} = \text{ifft}(\mathbf{X}, 2L', 2);$$

$$Z_{\max} = \max(\max(\text{abs}(\mathbf{Z}(:, 1:L))));$$

$$\mathbf{Z} = \mathbf{Z}(:, 1:L) / Z_{\max};$$

1. 3D array

The M sensor positions, relative to the first sensor position, are stacked into a matrix \mathbf{P} as defined in Eq. (23).

Algorithm 2: Creating sensor signals for an arbitrary 1D array that result from a spherical noise field.

Data: \mathbf{p}_x , M , L , N , f_s

Result: \mathbf{Z}

$$L' = 2^{\lceil \log_2(L) \rceil};$$

$$\omega = \pi f_s \left[0 : \frac{1}{L'} : 1 \right];$$

$$\phi = \arccos \left(1 - 2 \left[0 : \frac{1}{N-1} : 1 \right] \right);$$

for $k=1: N$ **do**

$$\mathbf{X}' = \text{randn}(1, L' + 1) + i \text{randn}(1, L' + 1);$$

$$\mathbf{X}(1, :) = \mathbf{X}(1, :) + \mathbf{X}';$$

for $m=2: M$ **do**

$$\Delta = \mathbf{p}_x(m) \cos(\phi(k));$$

$$\mathbf{X}(m, :) = \mathbf{X}(m, :) + \mathbf{X}' \exp(-j\Delta\omega/c);$$

end

end

$$\mathbf{X} = [\mathbf{X}(:, 1:L' + 1), \text{conj}(\mathbf{X}(:, L' : -1:2))];$$

$$\mathbf{Z} = \text{ifft}(\mathbf{X}, 2L', 2);$$

$$Z_{\max} = \max(\max(\text{abs}(\mathbf{Z}(:, 1:L))));$$

$$\mathbf{Z} = \mathbf{Z}(:, 1:L) / Z_{\max};$$

The path difference $\Delta(m, \phi)$ denotes the difference between the path lengths from the incident plane wave with direction ϕ to the m th sensor and the first sensor. Its value is calculated by projecting the position vector of the m th sensor on the x - y plane, and subsequently projecting the resulting position vector on the normal \mathbf{v} of the plane wave, i.e., $\Delta(m, \phi) = \mathbf{v}^T \mathbf{P}(:, m) / \|\mathbf{v}\|^2$. Since $\|\mathbf{v}\|^2 = 1$ we have

$$\Delta(m, \phi) = \mathbf{v}^T \mathbf{P}(:, m). \quad (19)$$

It should be noted that according to the model the height of the sensor does not influence the path difference.

The M sensor signals of length L that result from N uniformly distributed noise sources can be generated using Algorithm 3.

Algorithm 3: Creating sensor signals for an arbitrary 1D and 3D array that result from a cylindrical noise field.

Data: \mathbf{P} , M , L , N , f_s

Result: \mathbf{Z}

$$L' = 2^{\lceil \log_2(L) \rceil};$$

$$\omega = \pi f_s \left[0 : \frac{1}{L'} : 1 \right];$$

$$\phi = 2\pi \left[0 : \frac{1}{N} : \frac{N-1}{N} \right];$$

for $k=1: N$ **do**

$$\mathbf{X}' = \text{randn}(1, L' + 1) + i \text{randn}(1, L' + 1);$$

$$\mathbf{X}(1, :) = \mathbf{X}(1, :) + \mathbf{X}';$$

$$\mathbf{v} = \begin{bmatrix} \cos(\phi(k)) \\ \sin(\phi(k)) \\ 0 \end{bmatrix};$$

for $m=2: M$ **do**

$$\Delta = \mathbf{v}^T \mathbf{P}(:, m);$$

$$\mathbf{X}(m, :) = \mathbf{X}(m, :) + \mathbf{X}' \exp(-j\Delta\omega/c);$$

end

end

$$\mathbf{X} = [\mathbf{X}(:, 1:L' + 1), \text{conj}(\mathbf{X}(:, L' : -1:2))];$$

$$\mathbf{Z} = \text{ifft}(\mathbf{X}, 2L', 2);$$

$$Z_{\max} = \max(\max(\text{abs}(\mathbf{Z}(:, 1:L))));$$

$$\mathbf{Z} = \mathbf{Z}(:, 1:L) / Z_{\max};$$

2. 1D array

For an arbitrary 1D array the algorithm in Algorithm 3 can be simplified. Without loss of generality it is assumed that the sensors of the array are positioned on the x axis. All sensor positions are relative to the first sensor. The positions are stored in the vector \mathbf{p}_x as defined in Eq. (18).

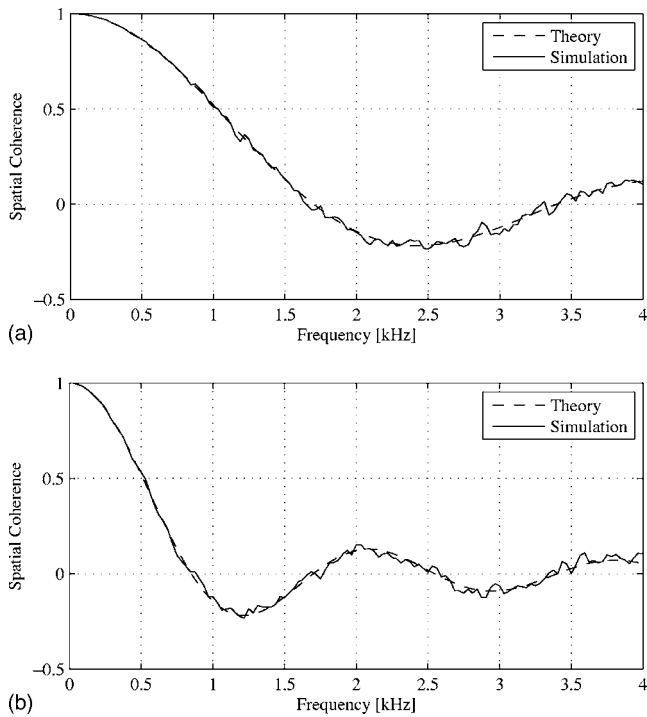


FIG. 4. Spatial coherence between two sensors with distance (a) $d=10$ cm and (b) $d=20$ cm, in a spherically isotropic noise field.

The M sensor signals of length L that result from N uniformly distributed noise sources can be generated by replacing the matrix \mathbf{P} by \mathbf{p}_x and by using

$$\Delta = \mathbf{p}_x(m)\cos(\phi(k)) \quad (20)$$

in Algorithm 3. Furthermore, the line containing the calculation of \mathbf{v} should be omitted.

IV. RESULTS

In this section we analyze the generated sensor signals. First, the obtained spatial coherence between two sensors in a spherical and cylindrical noise field is shown, and the number of noise sources N is investigated. Second, the number of noise sources N_ϕ and N_θ that are required for generating the sensor signals for a 3D array in a spherical noise field are investigated.

A. Using two sensors

First, the algorithm was used to generate the sensor signals in a spherically and cylindrically isotropic noise field using $N=64$ sources. We generated two sensor signals of $L=2^{18}$ samples and inter sensor distance $d=\{10, 20\}$ cm. The coherence between the two sensor signals was estimated using Welch's averaged periodogram method.¹⁰ We used a fast Fourier transform of length $K=256$, a Hanning window, and 75% overlap.

The simulation and theoretical results for the spherical and cylindrical noise fields are shown in Figs. 4 and 5, respectively. From the results shown in these figures we can see that the spatial coherence of the generated sensor signals closely matches the theoretical value.

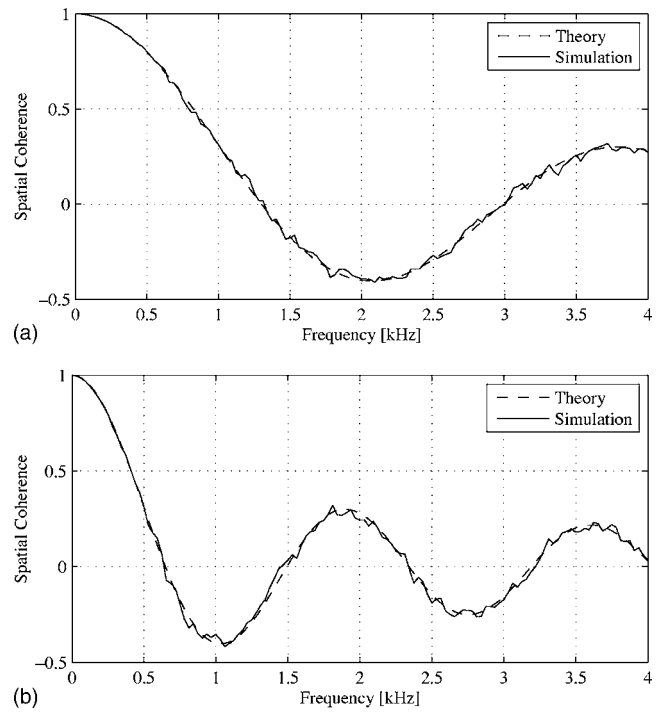


FIG. 5. Spatial coherence between two sensors with distance (a) $d=10$ cm and (b) $d=20$ cm, in a cylindrically isotropic noise field.

In practice only a finite set of noise sources can be used. Therefore, the theoretical value can only be approximated. The error between the spatial coherence of two generated sensor signals and theoretical spatial coherence is determined by i) the spectrum estimation error, and ii) the fact that a finite number of noise sources is used. The number of noise sources that is required will now be investigated. The error between the spatial coherence of two generated signals and the theoretical spatial coherence is defined by the normalized mean square error (MSE) between these two values, i.e.,

$$\text{MSE}(N) = \frac{\sum_{k=0}^{K/2} (\hat{\gamma}_{x_1 x_2}(k; N) - \gamma_{x_1 x_2}(k))^2}{\sum_{k=0}^{K/2} (\gamma_{x_1 x_2}(k))^2}, \quad (21)$$

where k denotes the discrete frequency index, and $\hat{\gamma}_{x_1 x_2}(k; N)$ denotes the estimated spatial coherence obtained using N noise sources. The results for a spherical and cylindrical noise field are shown in Figs. 6(a) and 6(b), respectively. For large N the MSE asymptotically reaches a level determined by the power spectral density estimation method. In case the number of noise sources is larger than approximately 64, the theoretical spatial coherence is well approximated.

B. Using three sensors

In this section the number of noise sources that is required for generating the sensor signals of a 3D array in a spherical noise field is investigated. The number of noise sources is specified by $N_\phi N_\theta$, where N_ϕ denotes the number of noise sources on each ring and N_θ denotes the number of rings. The average error between all unique spatial coherence

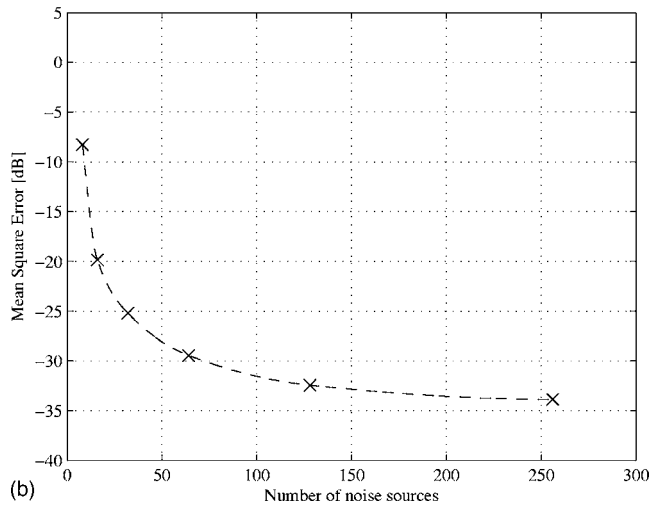
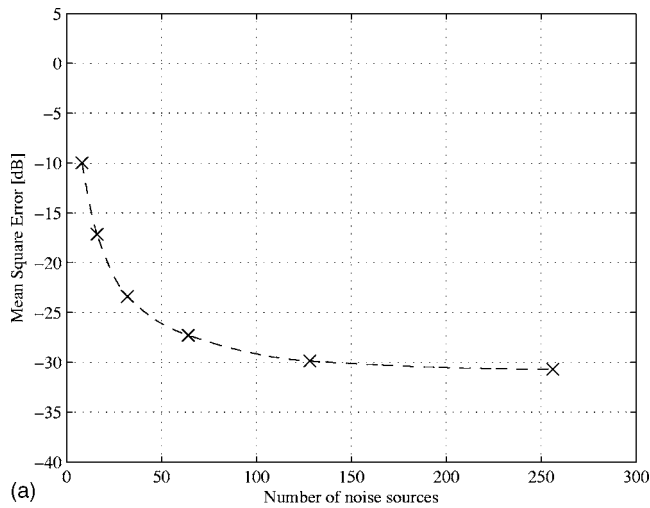


FIG. 6. MSE between the spatial coherence of the generated sensor signals and the theoretical value using N uncorrelated noise sources.

pairs of M generated sensor signals (obtained using Algorithm 1) and the corresponding theoretical spatial coherence values is obtained by

$$\text{MSE}(N_\phi, N_\theta) = \frac{2(M-2)!}{M!} \sum_{i=1}^M \sum_{j=i+1}^M \frac{\sum_{k=0}^{K/2} (\hat{\gamma}_{x_i x_j}(k; N_\phi, N_\theta) - \gamma_{x_i x_j}(k))^2}{\sum_{k=0}^{K/2} (\gamma_{x_i x_j}(k))^2}. \quad (22)$$

The position matrix of the three sensors that was used in this experiment is

$$\mathbf{P} = \begin{bmatrix} 0 & 0.2 & 0 \\ 0 & 0 & 0.2 \\ 0 & 0 & 0 \end{bmatrix}. \quad (23)$$

The contour plot of the average MSE obtained for different values N_ϕ and N_θ is shown in Fig. 7. From the results shown in this figure it can be concluded that both N_ϕ and N_θ should be sufficiently large to accurately generate the signals. In general $N_\phi \geq 96$ and $N_\theta \geq 32$ yield accurate results ($\text{MSE} < -25$ dB).

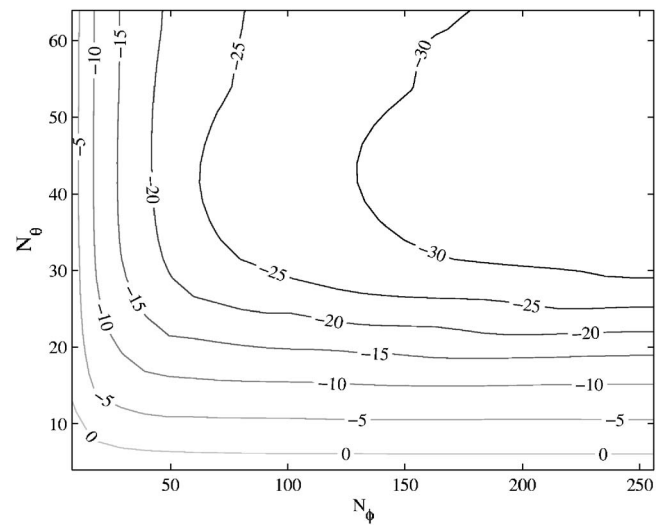


FIG. 7. Contour plot of $\text{MSE}(N_\phi, N_\theta)$ using $N_\phi N_\theta$ uncorrelated noise sources.

V. ACOUSTIC SIGNAL PROCESSING EXAMPLE

To demonstrate the applicability of the proposed simulator we use the generated sensor signals to verify the theoretical gain of a filter and sum beamformer in a spherically isotropic noise field.

The array gain of the filter and sum beamformer in a spherically isotropic noise field is equal to the directivity index (DI) of the array, which is given by¹¹

$$\text{DI}(k) = 10 \log_{10} \left(\frac{|\mathbf{w}(k)^H \mathbf{d}(k)|^2}{\mathbf{w}(k)^H \mathbf{\Gamma}_{\text{diffuse}}(k) \mathbf{w}(k)} \right) [\text{dB}], \quad (24)$$

where the numerator represents the power of the signal at the output of the beamformer, the denominator represents the power of the noise at the output of the beamformer, $\mathbf{\Gamma}_{\text{diffuse}}(k)$ denotes the spatial noise covariance matrix, $\mathbf{d}(k)$ denotes the (frequency dependent) array steering vector, and

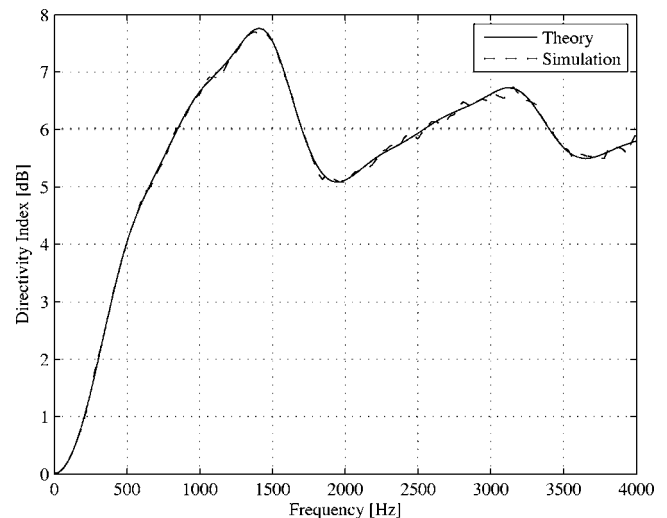


FIG. 8. Theoretical and simulated directivity index (DI) of a filter and sum beamformer and a uniform linear microphone array that consists of four microphones and an inter-microphone spacing of 0.2 m.

$\mathbf{w}(k)$ contains the frequency dependent weights of the beamformer.

Let us assume that the array steering vector of length M is $\mathbf{d}(k)=[1 \dots 1]^T \forall k$, and that $\mathbf{w}(k)=[1 \dots 1]^T \forall k$. It is easy to verify that for low frequencies ($k \rightarrow 0$) DI is equal to $10 \log_{10}(M^2/M^2)=0$ dB, and for high frequencies ($k \rightarrow K/2$) DI is equal to $10 \log_{10}(M^2/M)=10 \log(M)$ dB.

For this experiment a uniform linear microphone array was used. The number of microphones M equals 4, and the inter-microphone distance was 0.2 m. In Fig. 8 the theoretical DI, and the DI that was calculated using the generated sensor signals is shown. From the depicted results we can see that the generated sensor signals are applicable for verifying the theoretical performance of the beamformer.

VI. CONCLUSIONS

In this paper we have developed efficient algorithms to generate the sensor signals of a 1D and 3D array that are observed in a spherically or cylindrically isotropic noise field. The MATLAB implementation of the developed algorithms is available online.¹² It should be noted that the developed algorithms can be extended to a more general case in which directional sensors are used. This can be done by weighting the level of each of the source signals.^{1,5,7}

¹G. Elko, *Acoustic Signal Processing for Telecommunication*, edited by S. Gay and J. Benesty (Kluwer Academic, Hingham, MA, 2000), Chap. 10, pp. 181–237.

²I. McCowan and H. Bourlard, “Microphone array post-filter for diffuse noise field,” in *Proc. of the IEEE International Conference on Acoustics, Speech, and Signal Processing (ICASSP’02)*, 2002, Vol. 1, pp. 905–908.

³S. Gannot and I. Cohen, “Speech enhancement based on the general transfer function GSC and postfiltering,” *IEEE Trans. Speech Audio Process.* **12**, 561–571 (2004).

⁴N. Dal-Degan and C. Prati, “Acoustic noise analysis and speech enhancement techniques for mobile radio applications,” *Signal Process.* **18**, 43–56 (1988).

⁵G. Elko, *Microphone Arrays: Signal Processing Techniques and Applications*, edited by M. Brandstein and D. Ward (Springer, New York, 2001), Chap. 4, pp. 61–85.

⁶M. G. J. Bird, “Speech enhancement for mobile telephony,” *IEEE Trans. Veh. Technol.* **39**, 316–326 (1990).

⁷H. Cox, “Spatial correlation in arbitrary noise fields with application to ambient sea noise,” *J. Acoust. Soc. Am.* **54**, 1289–1301 (1973).

⁸R. Cook, R. Waterhouse, R. Berendt, S. Edelman, and M. Thompson, “Measurement of correlation coefficients in reverberant sound fields,” *J. Acoust. Soc. Am.* **27**, 1072–1077 (1955).

⁹L. Devroye, *Non-Uniform Random Variate Generation* (Springer-Verlag, New York, 2005), Chap. 2, p. 29.

¹⁰P. Stoica and R. Moses, *Spectral Analysis of Signals* (Prentice-Hall, Englewood Cliffs, NJ, 2005).

¹¹H. V. Trees, *Optimum Array Processing*, Detection, Estimation and Modulation Theory (Wiley, New York, 2002).

¹²E. Habets and S. Gannot, “Matlab implementation for: Generating sensor signals in isotropic noise fields,” url: <http://home.tiscali.nl/ehabets/ginfs.html> (last viewed September, 2007).